J. Eur. Opt. Society-Rapid Publ. 2025, **21**, 4

https://doi.org/10.1051/jeos/2024049
Available online at: https://jeos.edpsciences.org

Journal of the European Optical Society-Rapid Publications

RESEARCH ARTICLE OPEN ACCESS

Fast simulation of the influence of a refractive free-form microstructure on a wave field based on scalar diffraction theory

Fabian Thiemicke[1,2,*], Ramy El-Bashar[3,4], Mohamed F.M. Hameed[5,6], Mostafa Agour[1,7], Salah S.A. Obayya[4,8], Ralf B. Bergmann[1,9], and Claas Falldorf[1]

[1] BIAS-Bremer Institut für angewandte Strahltechnik, Klagenfurter Str. 5, 28359 Bremen, Germany
[2] University of Bremen, Faculty of Physics and Electrical Engineering, Otto-Hahn-Allee 1, 28359 Bremen, Germany
[3] National Institute of Laser Enhanced Sciences (NILES), Cairo University, 12613 Giza, Egypt
[4] Centre for Photonics and Smart Materials, Zewail City of Science, Technology and Innovation, October Gardens, 6th of October City, 12578 Giza, Egypt
[5] Center for Nanotechnology, Zewail City of Science, Technology and Innovation, October Gardens, 6th of October City, 12578 Giza, Egypt
[6] Mathematics and Engineering Physics Department, Faculty of Engineering, University of Mansoura, 35516 Mansoura, Egypt
[7] Faculty of Science, Department of Physics, Aswan University, 81528 Aswan, Egypt
[8] Electronics and Communications Engineering Department, Faculty of Engineering, University of Mansoura, 35516 Mansoura, Egypt
[9] University of Bremen, MAPEX Center for Materials and Processes and Faculty of Physics and Electrical Engineering, Otto-Hahn-Allee 1, 28359 Bremen, Germany

Received 7 November 2024 / Accepted 16 December 2024

Abstract. We present a novel fast simulation approach to simulate the influence of refractive freeform microstructures on a wave field. The FRISP (Finite Refractive Index Selective Propagation) method combines the Rayleigh-Sommerfeld diffraction integral with a thin element approximation and provides a comprehensive framework for understanding the optical properties of these microstructures. The main advantage of this method is its reduced complexity, which leads to a remarkable reduction in computation time by more than two orders of magnitude compared to finite-difference time-domain (FDTD) methods. This efficiency facilitates the iterative optimization of refractive microstructures and thus represents a practical tool to improve this type of microstructures. The verification of the FRISP method is realized by comparing the focal position and spot size of refractive microstructures. For this purpose, we compare FDTD, Mie theory and experimental data on microspheres with the predictions of FRISP. This comparison demonstrates the robustness and reliability of the approach, emphasizes its validity and demonstrates it as a valuable tool for the design and analysis of microstructures.

Keywords: Refractive micro structure, Scalar diffraction, Nanojet, Wave field propagation.

1 Introduction

In the field of nanophotonics, the precise control and manipulation of light is of key relevance. Here, photonic nanojets represent a well described and demonstrated method of diffracting light below the classical diffraction limit [1–3]. For the generation of photonic nanojets, typically dielectric microspheres or other nanostructures are used. In order to understand and realize photonic nanojets' potential, sophisticated and time-efficient simulation techniques play a crucial role. The simulation of photonic nanojets is typically based on a numerical solution of Maxwell's equations. In the case of spherical elements, Mie theory [4] offers a suitable and efficient basis for understanding the interaction of light with circular symmetric dielectric structures and the formation of photonic nanojets [5, 6]. Microstructures which are not spherical require more involved methods such as Finite-Difference Time-Domain (FDTD) simulation [1, 7, 8]. The shape of microstructures is a significant parameter for the properties of photonic nanojets, especially in terms of the size and position of the focus spot of the nanojet [6, 8–10]. For the purpose of shape optimization it would be very important to simulate a large number of different geometries in a short time and optimize the shape of the micro structures to achieve the expected properties. As explained above, Mie theory is limited to circular symmetric structures [5]. In the case of more complex structures or cylinders, usually FDTD methods are used to solve Maxwell's equations. A disadvantage of these methods is the high computational effort and the resulting computation times of several hours for each structure [11]. The approach is thus not practical for numerical

* Corresponding author: thiemicke@bias.de

optimization procedures that employ a significant amount of parameter variations.

In this paper, we present a novel approach for the fast simulation of the influence of a refractive free-form micro structure on a wave field based on scalar diffraction theory. Our approach is based on the Rayleigh-Sommerfeld diffraction integral which is a powerful tool to exactly calculate the propagation of wave fields even in the near field regime. We also incorporate a thin element approximation to the diffraction integral, to propagate the wave field through successive slices of the refractive element. The method allows us to predict the wave field in the near-field region of the refractive elements. Additionally, by incorporating the thin element approximation, we can simplify the mathematical complexity of the problem, making the method more accessible for practical applications. Our approach therefore provides a reduced computational time compared to conventional methods such as Mie theory and FDTD-simulations.

In order to demonstrate the suitability of the FRISP approach, comparisons with simulations of photonic nanojets shown in the literature based on FDTD-simulations [8, 12] and measurements on real micro-spheres are shown. Due to the reduced computation time, the effect of deviations between the desired and the real geometry of microstructures can be determined using suitable parameter studies.

2 Scalar diffraction theory applied to micro structures

2.1 Modeling

The FRISP approach is based on scalar diffraction theory, in which the propagation can be described by the Rayleigh-Sommerfeld diffraction integral [13]. The validity of the scalar diffraction theory for determining the focusing properties of microstructures is based on the assumptions that the microstructures have a homogeneous predefined refractive index distribution and that the focusing properties are independent from polarization (birefringence). The Rayleigh-Sommerfeld diffraction integral can be used to calculate the near-field behavior of light when it interacts with apertures, lenses or refractive elements using [13]

$$U(x,y) = \frac{1}{i\lambda z}\iint_{-\infty}^{\infty} \frac{U(x',y')e^{-ikr}}{r}\cos\theta\, dx'\, dy', \qquad (1)$$

where $U(x, y)$ is the complex amplitude of the diffracted field at the observation plane, $U(x', y')$ is the complex amplitude of the source field, λ is the wavelength of the light, z is the distance from the source to the observation plane, x', y' are the coordinates of the source field, x, y are the coordinates of the observation point, $r = \sqrt{(x-x')^2 + (y-y')^2 + z^2}$ is the distance between the observation point and the point on the source plane, $k = 2\pi/\lambda$ is the wave number and θ the angle between the wave vector and the z-axis with which the source field arrives at the image plane. The near-field zone can include any propagation distance between the evanescent field region and several wavelengths. The Rayleigh-Sommerfeld diffraction integral may be challenging to solve in a closed-form solution, but it can be solved numerically using methods such as the fast Fourier transform (FFT) [14] or assuming suitable boundary conditions to simplify the calculations [15].

In our case, the solution of the Rayleigh-Sommerfeld diffraction integral is calculated by a plane wave decomposition without the use of any simplifications apart from the assumptions described above. As the propagation distance is in a range of $\Delta z \ll \lambda$, we can not use the Fresnel approximation. The plane wave decomposition for the free-space propagation is calculated via the transfer function in the frequency domain

$$H(v_x, v_y) = \exp\left[i\,2\pi\,\Delta z\sqrt{\frac{1}{\lambda^2} - v_x^2 - v_y^2}\right], \qquad (2)$$

where v_x and v_y are the spatial frequencies, λ the wavelength of the light and Δz the propagation distance [13]. As a result of the very small propagation distances and thus the evanescent waves we are dealing with, no cutoff frequency occurs as in the case of propagation with $\Delta z \gg \lambda$. The transfer function does therefore not only account for the propagation of far field modes but also evanescent field components. Determining the transfer function in frequency space makes it easy to choose the field components that are taken into account in the calculation by filtering space frequencies using high-pass, low-pass, or band-pass filters [13]. This procedure enables us to calculate and evaluate only the propagation of evanescent field components. Furthermore, this procedure can be used for the evaluation of the optical properties of the simulated structures, especially for an optimization of the shape of the surface. However, there are limitations compared to FDTD or Mie theory-based simulations, because back scattering effects are not considered in scalar diffraction theory and thus cannot be described in the proposed approach.

2.2 Calculation of wave propagation using 2D-slicing of 3D-structures

In order to compute the effect of a 3-dimensional (3D) dielectric micro structure on a wavefront with scalar diffraction theory methods, the model domain is divided into separate layers with a layer thickness $\Delta z \ll \lambda$. Figure 1(a) shows a schematic illustration of the segmentation of the 3D simulation environment into M layers (b) and the calculation sequence for a layer with 2 different refractive indices n_0 and n_1.

The numerical calculation of the Rayleigh-Sommerfeld diffraction integral subsequently determines the effect of these layers on the wavefront. The effect on the wavefront is determined for all refractive indices separately and then the resulting wavefront for the entire layer is compiled according to the regions with different refractive indices. For each occurring refractive index, the propagation over the distance Δz is determined by free space propagation for this layer. Then the result of this propagation is assigned to the area inside the layer that corresponds to this refractive index. The procedure is repeated for all refractive

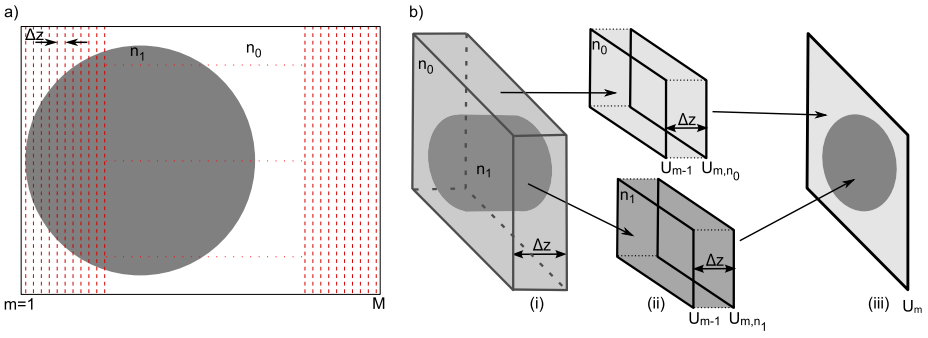

Figure 1. Schematic representation of the calculation of the wavefront for a dielectric microsphere. a) Slicing the simulation volume with a micro sphere with refractive index n_1 in an environment with n_0 into M separate layers with a thickness Δz. Scheme of the calculation of the wave front U_m for a layer with 2 different refractive indices (n_0 and n_1). In (i) the regions with different refractive indices n_i are identified. The wavefront U_m-1 serves in (ii) as input wavefront and will be propagated over the distance Δz. The propagation is determined separately for each refractive index (n_0 and n_1) resulting in the wavefronts U_m, n_0 and U_m, n_1. Finally, these wavefronts will be combined in (iii) to U_m.

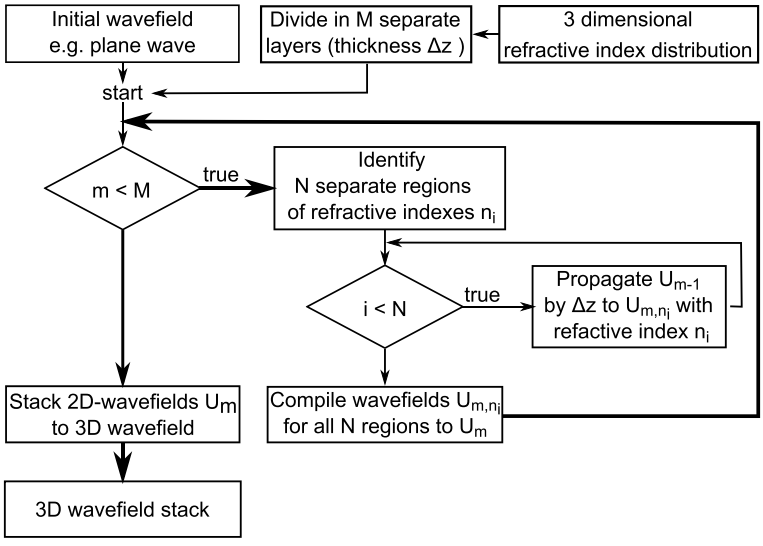

Figure 2. Flowchart of the simulation of a 3D microstructure with N different refractive indices n_i and M layers with a layer thickness Δz. During the calculation of the 3D wave front stack, there are 2 loops. The outer loop (bold lines) represents the propagation of the M layers (see Fig. 1a)). The inner loop is used to calculate the wavefront U_m with several refractive indices n_i (see Fig. 1b)).

indices to calculate the wavefront behind the actual layer at the distance Δz. The individual refractive indices can also be complex and contain an individually defined absorption for each refractive index. An individual absorption was, however, not taken into account for the validation described in the following sections. The 2-dimensional (2D) wavefront is subsequently stored in a stack to generate the 3D wavefront information. This procedure is then repeated for all M layers. In each case, the wavefront of the previous layer is used as the input wavefront for the currently calculated layer.

Figure 2 shows a flow chart of the simulation of the entire structure and their influence on the wavefront. The calculation of the influence of the refractive index distribution on the wavefront is performed in two loops. An outer loop calculates the influence of a complete layer on the wavefront at a distance Δz while the inner loop calculates the influence of the different refractive indices inside the layer.

3 Simulation results and experimental verification

3.1 Intensity calculation and validation

To validate the introduced FRISP method for the computation of focusing properties of optical micro structures with a size in the single- to double-digit micrometer range by methods of coherent optics, a comparison of different simu-

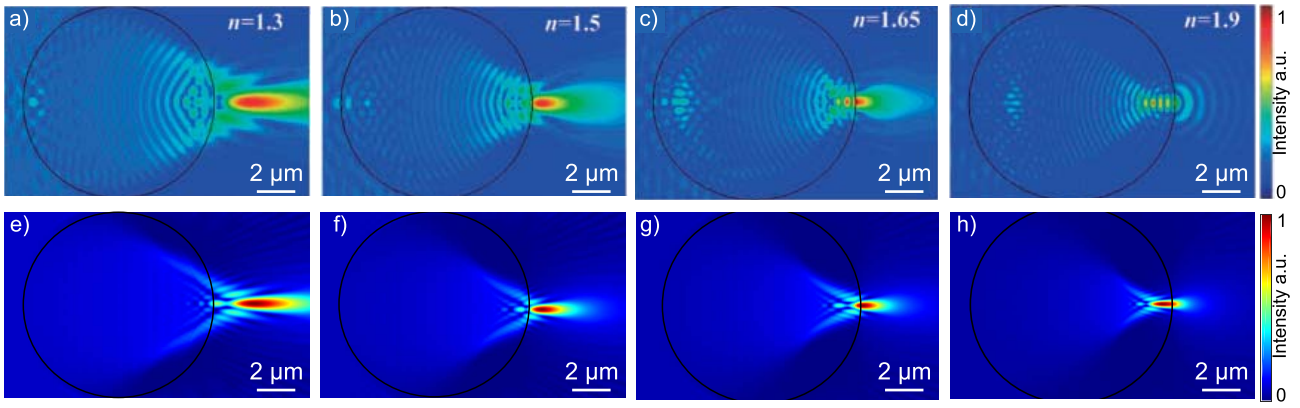

Figure 3. Comparison of the FRISP methode for the simulations based on Rayleigh-Sommerfeld diffraction followed by step-wise propagation and FDTD-simulations based on [12] (© 2018 The Japan Society of Applied Physics). a) to d) results of FDTD-simulations, e) to h) results of the FRISP method. Refractive index $n = 1.3$ for (a) and (e), $n = 1.5$ for (b) and (f), $n = 1.65$ for (c) and (g) and $n = 1.9$ for (d) and (f) of a microsphere with a diameter of 10 µm.

lations published in the literature is shown in the following. To validate the FRISP method, we started our analysis by using a microsphere characterized with a fixed diameter of 10 µm, while systematically varying its refractive index. This scenario, previously explored by Zhou et al. in their seminal paper [12], was investigated using FDTD simulation within the CST MWS software package.

Figure 3 visually compares results derived from the FDTD-based simulations in the paper from Zhou et al (a–d) and our approach (e–h) based on the Rayleigh-Sommerfeld diffraction integral and a layer-wise propagation. The visual representation in the figure shows a striking consistency for the focal width and position of the focal spot between the two methods. This compelling agreement underscores the effectiveness and accuracy of the FRISP approach in capturing the intricate optical nuances associated with microsphere behavior. However, it is important to note one difference between the simulations. The FRISP approach lacks the capability of describing backward propagation. This limitation manifests itself as a loss of energy at the boundaries of the microsphere, which prevents the method from calculating the interference pattern of the backscattered light within the sphere. The influence on the energy caused by the disregard of reflections can be estimated by observations of refractive index transition. For typical refractive index differences, the losses due to reflections are in the lower single-digit percentage range per interface. Despite this difference, the overall congruence in the essential focal characteristics highlights the practicability of our method in realistically representing the optical behavior of the microstructures.

In order to prove the validity of the FRISP method for different refractive indices, the results of the work by Lee et al. [16] based on the Mie theory were compared with the FRISP method. The comparison results for the FWHM are shown in Table 1. The deviations between the methods are less than 5% over a wide range of wavelengths and refractive indices, which demonstrates the validity of the FRISP method.

Figure 4 illustrates the potential of the FRISP approach by showing simulation results of a pyramidal structure composed of two different materials. a) Shows a schematic sketch of the simulated microstructure with 2 different materials, b) shows the result of an FTDT simulation by Ge et al. [8] while c) shows the result of the FRISP method. A comparative analysis with the simulation performed by Ge et al. [8] shows noticeable deviations in the intensity distribution within the pyramid structure, especially below the boundary layer separating the two materials. The significant refractive index contrast induces back reflection in the silicon nitrate. It's noteworthy that the FRISP approach, which lacks the capability for backpropagation, results in energy loss at the boundaries within the pyramid, specifically at the interface between silicon nitrate (left) and silicon dioxide (right). In addition, the absence of interference effects within the pyramid structure is a distinctive feature observed in our simulation, which distinguishes it from the simulation by Ge et al. These differences show the limitations of the FRISP method with respect to backscattering and backreflections. However, FRISP can be used to determine the position and shape of the nanojet generated by the microstructure.

3.2 Performance and computational time

In this study, we evaluate the computational effort associated with the FRISP method and compare it to finite-difference time-domain (FDTD) simulations [17]. The computational complexity of the FRISP approach depends primarily on factors such as the number of discrete layers, the pixel density per layer and the number of materials with different indices. The simulation domain, tailored to the typical scenario of studying photonic nanojets, spans dimensions of 25 µm × 25 µm × 25 µm, with two different refractive indices delineating the inside and outside regions of the microstructure. Using a mesh resolution of 50 nm × 50 nm × 50 nm, the computational time of the FRISP method implementation in MATLAB is less than 1 min. However, the FDTD based on the Ansys/Lumerical software package is used with a computational domain of 25 µm × 25 µm × 38 µm and a fixed mesh size of 50 nm. In addition, perfect matched layer (PML) boundary

Table 1. Comparison of the focus point FWHM and the error between Mie-theory based simulation [16] and FRISP-method for micro-spheres with a diameter of 5 µm, different refractive indices n and wavelength λ.

Refractive index n	Focus point with calculation method	λ [nm] 300	400	500	600
1.46	Mie-theory [nm]	198	256	285	354
	FRISP [nm]	198	254	290	351
	Deviation [%]	0.0	0.8	1.7	0.9
1.59	Mie-theory [nm]	177	220	275	330
	FRISP [nm]	176	222	271	319
	Deviation [%]	0.6	0.9	1.5	3.4
1.93	Mie-theory [nm]	126	160	195	216
	FRISP [nm]	128	162	197	223
	Deviation [%]	1.6	1.2	1.0	3.1
2.20	Mie-theory [nm]	102	120	150	186
	FRISP [nm]	103	125	157	187
	Deviation [%]	1.0	4.0	4.5	0.5

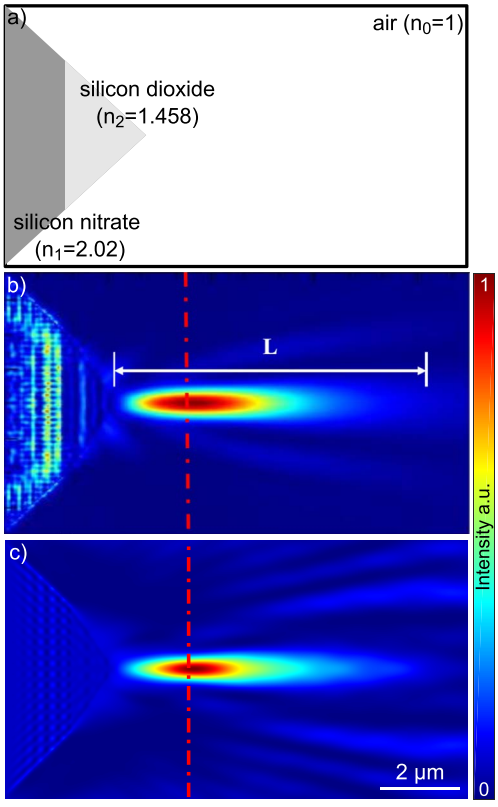

Figure 4. Comparison of the FRISP method for pyramidal microstructures consisting of two different materials. a) Schematic illustration of the composition of the microstructure. b) Simulation based on FDTD-simulation [8] (reproduced with permission from author) with L length of the nanojet and c) simulation based on the FRISP approach. The red line highlights the position of the highest intensity of the nanojet.

conditions are applied in all directions to reduce any boundary reflections [18]. To further reduce reflections, 8 layers of stretched coordinate PML are also used [19]. In this study, the computation time for the FDTD simulation is almost 5 h using an HP Z400 workstation with 20 GB RAM. To reduce the computation time, symmetric boundary conditions are used instead of PML as suggested in [20]. However, the calculation time is about 85 min. In contrast, the computational time of the proposed method with a non-optimized implementation in Matlab is only 38 s. Consequently, the proposed approach achieves a remarkable reduction in computational time with a factor of 135. This allows the use of (e.g. iterative) optimization methods that take into account the dependence of the transmitted field on the actual shape of the micro structure.

Figure 5 provides a comparison of the simulation results between the FRISP method and an FDTD simulation for a microsphere with a diameter of 10 µm and a refractive index of $n = 1.5$ and a wavelength of 634 nm. It may be seen that good agreement occurs between FRISP results and those obtained by the FDTD. The deviations in the intensity maps a) and b) for regions inside the sphere are due to the backscattering effects that are not captured by the FRISP approach. In order that the intensity distributions are still comparable, the intensities were normalized to their maximum in each case. However, the intensity distribution profiles between the two simulations show a very good agreement and almost identical sizes c) and positions d) of the focal spot. The focal spot is located at a distance of approximately 5.7 µm from the center of the micro sphere for both methods with a deviation of 2.2% between the FDTD simulation and the FRISP method. The deviation for the Full Width at Half Maximum (FWHM) of the focal spot is only 1% for a focal spot diameter of 399 nm in the shown example.

Table 2 shows the specific values for the position and FWHM of the focus spot for the example shown in Figure 5

Furthermore, the FRISP method does not require a complex preliminary consideration of the boundary conditions and the design of the perfectly matched layer environment, as is necessary for solving Maxwell's

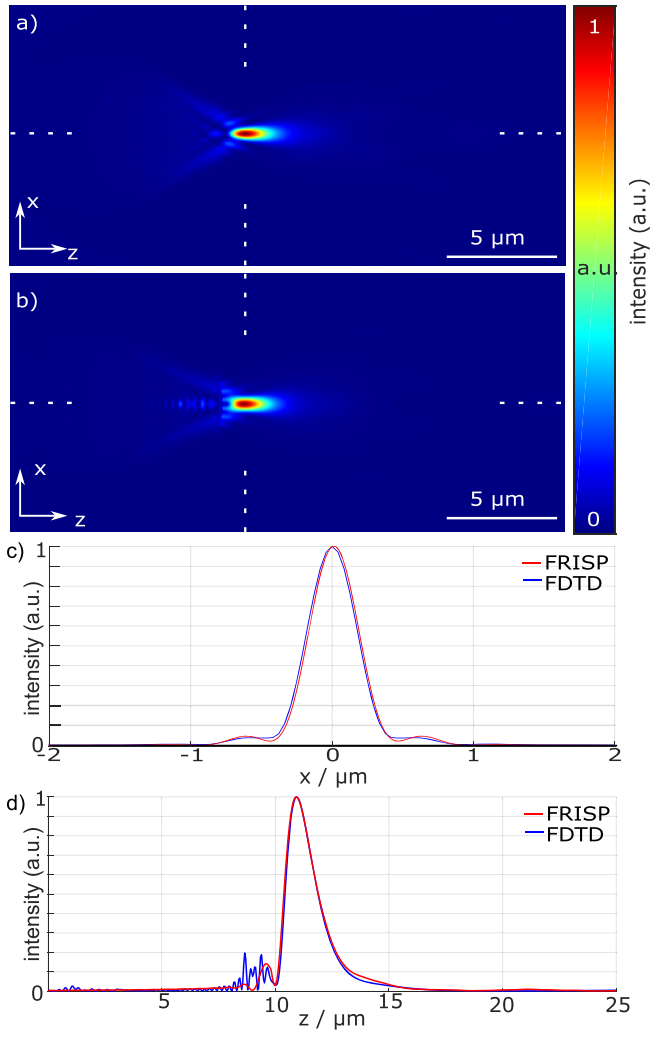

Figure 5. Comparison of the FRISP method with a FDTD simulation of a microsphere with a diameter of 10 µm, a refractive index of $n = 1.5$ and a wavelength of 634 nm. The normalized intensity distribution of a simulated photonic nanojets generated by the microsphere along the propagation axis a) for the FRISP method and b) for a FDTD simulation with Ansys. c) Comparison of the intensity profiles at the focal spot position along the vertical dashed lines to determine the FWHM. d) Intensity profiles along the horizontal dashed lines through the center of the micro sphere.

equations with the FDTD method [17]. This leads to additional time savings during the preparation of the simulation and simplifies the consideration of correlations between the shape of the micro structure and its intensity distribution.

3.3 Experimental validation

In addition to the comparison with simulation results obtained in the literature, we also compare the FRISP approach with experimental results from measurements of the focusing properties of SiO_2 micro spheres with a diameter of 11 µm. The measurement of the intensity

Table 2. Comparison of the FRISP method with FDTD simulation of a microsphere with a diameter of 10 µm and a refractive index of $n = 1.5$.

Method	Position focal spot [µm] from sphere center	Deviation of position [%]	FWHM [nm]	Deviation of FWHM [%]
FDTD	5.67	—	399	—
FRISP	5.8	2.2	396	1.0

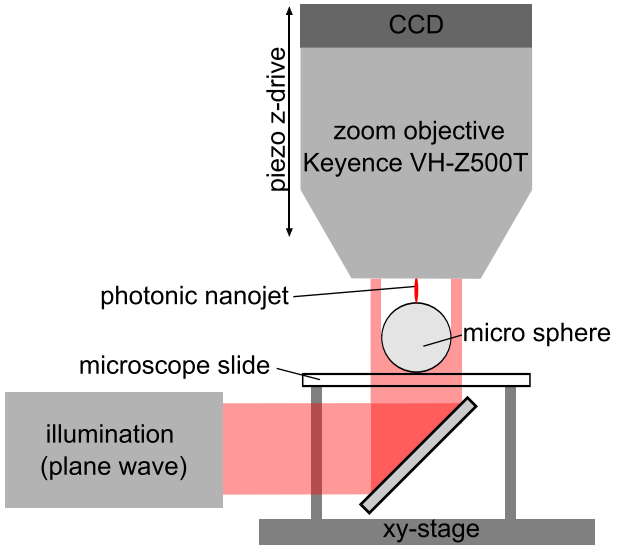

Figure 6. Schematic sketch of the optical setup for measuring the influence of a micro sphere on the intensity distribution of a plane wave.

distribution of the micro sphere was performed with a Keyence digital microscope *VHX*-7000 and a Keyence zoom objective VH-Z500T (zoom factor 5000 and $NA = 0.82$). For the illumination we used a laser diode (LP637-PA70) with a wavelength of 634 nm and a laser driver (CLD1010) from Thorlabs.

Figure 6 shows a schematic sketch of the optical setup for the measurement. The 3D intensity distribution consists of 200 separate 2D images with a vertical spacing of 85 nm. These images are then combined into a 3D stack of images. In order to correct for any lateral displacement of the images during the measurement process, a cross-correlation of the successive images was carried out.

Figure 7 shows the results of an experimental measurement and a simulation of a SiO_2 microsphere with a diameter of 11 µm. There is a strong similarity between the experimental and simulation results in terms of focal spot position and size. For areas inside the micro sphere there are some deviations between the simulated and measured intensity distribution. These deviations are caused by the effects of backscattering and reflection inside and at the boundaries of the micro sphere, which are not modeled by the FRISP approach. The similarity of the intensity distribution for the focal region of the microstructure confirms

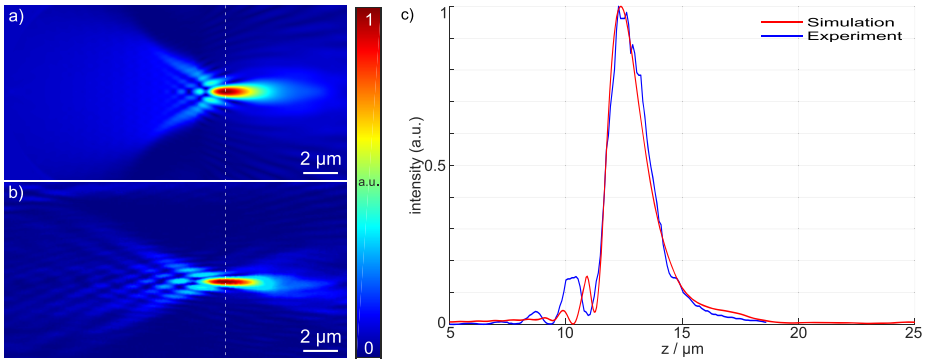

Figure 7. Experimental validation of the FRISP method with a SiO_2 micro sphere with a diameter of 11 µm. The normalized intensity distribution of a Photonic nanojet generated by a SiO_2 micro sphere along the propagation axis a) simulated and b) measured by an optical microscope. c) Comparison of the intensities along the centerline of the simulation a) (red) and the experiment b) (blue).

the validity of the FRISP approach for the simulation of photonic nanojets.

4 Conclusion

We present the FRISP method based on scalar diffraction theory which can simulate the focusing properties of microstructures with structure sizes <50 µm and the corresponding photonic nanojets in the focal plane of the structure. Compared with standard FDTD-simulations, the computing time for such simulations with the FRISP approach is reduced by a factor of 135 and a conventional desktop computer can be used. In contrast with the significantly more computational-intensive FDTD simulations, the FRISP method has the limitation that it does not consider back reflections. FRISP method calculates only the forward propagation of the light, which leads to a deviation of the results between the FRISP method and FDTD simulations inside the microstructures. For regions outside the structure, especially for the shape, width (FWHM) and position of the focal spot, the FRISP method shows very good agreement with FDTD simulations. The errors for the focus position are in the range of 2.2% and for the FWHM in the range of 1%.

Consequently, the FRISP approach appears very suitable for the efficient simulation and iterative optimization of the focusing properties of optical micro structures, especially with respect to the geometry of photonic nanojets and near-field applications. Referring to [21, 22], we aim to extend the FRISP method in future work to incorporate the analysis of backward reflecting waves.

Acknowledgments

The authors are grateful to Reiner Klattenhoff (BIAS) for his technical support with the optical setup and experimental work.

Funding

The authors gratefully acknowledge the support of the Deutsche Forschungsgemeinschaft (DFG, German Research Foundation) for funding this work under the project "Hochauflösende optische Mikroskopie mittels transmissiver Mikrostrukturen – HOMiTrans", grant no. 431605610.

Conflicts of interest

The authors declare no conflicts of interest.

Data availability statement

The Data underlying the presented results and the used Matlab algorithms may be obtained from the authors upon a reasonable request.

Author contribution statement

Conceptualization, F.T. and C.F.; Data curation, F.T., M.A., R.E.B., M.F.O.H. and C.F.; Investigation, F.T., M.A., R.E.B. and M.F.O.H.; Methodology, F.T., M.A. and C.F.; Validation, F.T., M.A., R.E.B., M.F.O.H. and C.F.; Visualization, F.T., M.A., R.E.B. and M.F.O.H.; Formal Analysis,F.T., M.A., R.E.B., M.F.O.H. and C.F.; Writing—original draft, F.T., and C.F.; Funding acquisition, R.B.B.; Supervision, S.S.A.O, R.B.B. and C.F. All authors have read and agreed to the submitted version of the manuscript.

References

1 Chen Z, Taflove A, Backman V, Photonic nanojet enhancement of backscattering of light by nanoparticles: a potential novel visible-light ultramicroscopy technique, *Opt. Express* **12**, 7, 1214–1220 (2004). https://doi.org/10.1364/OPEX.12.001214.
2 Heifetz A, Kong SC, Sahakian AV, Taflove A, Backman V, Photonic nanojets, *J. Comput. Theor. Nanosci.* **6**, 9, 1979–1992 (2009). https://doi.org/10.1166/jctn.2009.1254.
3 Darafsheh A, Photonic nanojets and their applications, *J. Phys. Photon.* **3**, 2, 022001 (2021). https://doi.org/10.1088/2515-7647/abdb05.
4 Wriedt T, Mie theory: a review, in *The Mie Theory: Basics and Applications* (Springer Berlin, Heidelberg, Germany, 2012), pp. 53–71.
5 Hulst HC, van de Hulst HC, *Light Scattering by Small Particles* (Courier Corporation, New York, 1981).
6 Luk'yanchuk BS, Paniagua-Domínguez R, Minin I, Minin O, Wang Z, Refractive index less than two: photonic nanojets yesterday, today and tomorrow, *Opt. Mater. Express* **7**, 6, 1820–1847 (2017). https://doi.org/10.1364/OME.7.001820.
7 Taflove A, Oskooi A, Johnson SG, *Advances in FDTD Computational Electrodynamics: Photonics and Nanotechnology* (Artech House, Norwood, Massachusetts, 2013).

8 Ge S, Liu W, Zhang J, Huang Y, Xi Y, Yang P et al., Novel bilayer micropyramid structure photonic nanojet for enhancing a focused optical field, *Nanomaterials* **11**, 8, 2034 (2021). https://doi.org/10.3390/nano11082034.

9 Minin IV, Minin OV, Geints YE, Localized EM and photonic jets from non-spherical and non-symmetrical dielectric mesoscale objects: brief review, *Annalen der Physik* **527**, 7–8, 491–497 (2015). https://doi.org/10.1002/andp.201500132.

10 Geints YE, Minin IV, Panina EK, Zemlyanov AA, Minin OV, Comparison of photonic nanojets key parameters produced by nonspherical microparticles, *Opt. Quantum Electron.* **49**, 1–7 (2017). https://doi.org/10.1007/s11082-017-0958-y.

11 Śliwak A, Jeleń M, Patela S, Modelling and analysis of fibre microlenses with ray-tracing and finite-difference methods, *Opto-Electron. Rev.* **30**, e140147 (2022). https://doi.org/10.24425/opelre.2022.140147.

12 Zhou Y, Tang Y, He Y, Liu X, Hu S, Effects of immersion depth on super-resolution properties of index-different microsphere-assisted nanoimaging, *Appl. Phys. Express* **11**, 3, 032501 (2018). https://doi.org/10.7567/APEX.11.032501.

13 Goodman JW, *Introduction to Fourier Optics* (Roberts and Company Publishers, Englewood, Colorado, 2005).

14 Shen F, Wang A, Fast-Fourier-transform based numerical integration method for the Rayleigh-Sommerfeld diffraction formula, *Appl. Opt.* **45**, 6, 1102–1110 (2006). https://doi.org/10.1364/AO.45.001102.

15 Sherman GC, Application of the convolution theorem to Rayleigh's integral formulas, *JOSA* **57**, 4, 546–547 (1967). https://doi.org/10.1364/JOSA.57.000546.

16 Lee S, Li L, Wang Z, Optical resonances in microsphere photonic nanojets, *J. Opt.* **16**, 1, 015704 (2013). https://doi.org/10.1088/2040-8978/16/1/015704.

17 Bérenger JP, *Perfectly Matched Layer (PML) for Computational Electromagnetics* (Springer Nature, Cham, 2022).

18 Ansys. PML boundary conditions in FDTD and MODE. [Retrieved 07 Nov. 2024], https://optics.ansys.com/hc/en-us/articles/360034382674-PML-boundary-conditions-in-FDTD-and-MODE.

19 Gedney SD, Zhao B, An auxiliary differential equation formulation for the complex-frequency shifted PML, *IEEE Trans. Antennas Propag.* **58**, 3, 838–847 (2009). https://doi.org/10.1109/TAP.2009.2037765.

20 Ansys. Symmetric and anti-symmetric BCs in FDTD and MODE. [Retrieved 07 Nov. 2024], https://optics.ansys.com/hc/en-us/articles/360034382694-Symmetric-and-anti-symmetric-BCs-in-FDTD-and-MODE.

21 Obayya S, Novel finite element analysis of optical waveguide discontinuity problems, *J. Lightwave Technol.* **22**, 5, 1420–1425 (2004). https://doi.org/10.1109/JLT.2004.827671.

22 Said AM, Heikal A, Areed NF, Obayya S, Why do field-based methods fail to model plasmonics? *IEEE Photon. J.* **8**, 5, 1–13 (2016). https://doi.org/10.1109/JPHOT.2016.2600367.